

# Fluorosis Induces Endoplasmic Reticulum Stress and Apoptosis in Osteoblasts In Vivo

Lu Liu · Ying Zhang · Hefeng Gu · Kaiqiang Zhang · Lin Ma

Received: 17 August 2014 / Accepted: 20 November 2014 / Published online: 2 December 2014  
© Springer Science+Business Media New York 2014

**Abstract** The present study investigated the effects of fluoride on endoplasmic reticulum (ER) stress (ERS) and osteoblast apoptosis in vivo. Forty-eight Wistar rats were randomly divided into four groups (12/group) and exposed to 0, 50, 100, and 150 mg/L of fluoride in drinking water for 8 weeks, respectively. Peripheral blood samples and bilateral femurs were used to monitor the progression of fluorosis in the animals. Hematoxylin and eosin (H&E) staining of the bone tissues was used to determine the severity of osteofluorosis. The expression of ERS chaperones (glucose-regulated protein 78 (GRP78), X-box binding protein 1 (XBP1), cysteine aspartate specific protease-12 (caspase-12), and growth arrest and DNA damage-inducible gene 153 (Gadd153/CHOP) was analyzed by immunohistochemistry staining, and osteoblast apoptosis was determined by TUNEL staining and flow cytometry. Accumulation of fluoride in bone was associated with the severity of osteofluorosis. The expression of GRP78, XBP1, caspase-12, and CHOP was increased in a dose-dependent manner. Fluoride-induced apoptosis in osteoblasts was also dose-dependent. High concentrations of fluoride induced ERS and osteoblast apoptosis in vivo. The increased expression of GRP78 and XBP1 increased the adaptation of osteoblasts to ERS to a certain extent. Caspase-12 and CHOP activation was associated with ERS and osteoblast apoptosis.

**Keywords** Endemic fluorosis · Osteoblast · Apoptosis · Unfolded protein response (UPR) · Osteofluorosis · ERS chaperones

## Introduction

Fluoride, a trace element, plays an important role in the deposition of calcium and phosphorus in the bones [1]. However, excessive fluoride can cause fluorosis, and fluoride poisoning has been a serious public health problem in many parts of the world [2–4].

Fluoride is often accumulated in the bones and teeth [4, 5]. Osteofluorosis is a typical sign of chronic fluorosis, exhibiting osteomalacia, bone sclerosis, osteoporosis, and heterotopic ossification [4, 6]. In recent years, there has been increasing evidence supporting the hypothesis that increased osteoblast activity and accelerated bone turnover are characteristics of the pathogenesis of osteofluorosis [7, 8]. However, the underlying molecular mechanisms remain largely unknown.

Epidemiological studies have suggested that endemic fluorosis is a calcium paradox disease closely related to malnutrition in dietary calcium [9]. In patients with endemic fluorosis, whole body calcium is decreased, but the intracellular concentration of  $\text{Ca}^{2+}$  is increased [10]. Chronic fluoride poisoning can open  $\text{Ca}^{2+}$  channels in osteoblasts and lead to intracellular calcium overload [11, 12]. The endoplasmic reticulum (ER) is largely responsible for calcium homeostasis and calcium signal transduction [13–15]. Changes in ER  $\text{Ca}^{2+}$  channels and  $\text{Ca}^{2+}$  homeostasis (calcium deprivation or calcium overload) can affect the function of the ER, leading to the accumulation of unfolded and misfolded proteins in the ER lumen and causing ER stress (ERS) [13–16]. This in turn leads to the unfolded protein response (UPR) or the downregulation of a series of specific genes associated with transcription and protein translation [17]. Protein synthesis is halted to reduce the ER load. If ER function cannot be restored, cell apoptosis often occurs [14, 15, 18, 19]. Molecular signals involved in ERS and UPR are associated with osteofluorosis and may activate apoptotic signals.

L. Liu · Y. Zhang (✉) · H. Gu · K. Zhang · L. Ma  
Department of Preventive Dentistry, School of Stomatology, China Medical University, ShenYang, China  
e-mail: zhangyingcmu@vip.163.com

The glucose-regulated protein 78 (GRP78), X-box binding protein 1 (XBP1), cysteine aspartate specific protease-12 (caspase-12), and growth arrest and DNA damage-inducible gene 153 (Gadd153/CHOP) are important ERS chaperones [20]. Under normal physiological conditions, GRP78 forms heterodimers with three transmembrane receptors, IRE1, PERK, and ATF6, on the ER membrane [20–22]. When ERS is induced, GRP78 dissociates with transmembrane receptors, promoting UPR [23]. XBP1, which belongs to the CREB/ATF protein family, is a basic leucine zipper protein and is widely expressed in mammalian cells, especially in liver cells [24]. It plays an important role in restoring  $Ca^{2+}$  homeostasis in the ER [25]. Under ERS, *XBP1* mRNA is induced by ATF6 and spliced by IRE1, producing a highly active transcription factor, XBP1s, which promotes ER-associated protein degradation (ERAD) and UPR [26]. Caspase-12, a member of cysteine aspartate kinase family, is expressed only in the ER [27]. Under ERS, caspase-12 is specifically activated, disturbing  $Ca^{2+}$  homeostasis and causing the accumulation of misfolded proteins in the lumen of the ER. This activates caspase-9 and caspase-3, eventually inducing cell apoptosis [27, 28]. CHOP is an important marker for ERS [29]. Under normal physiological conditions, the expression of CHOP is maintained at a relative low level. When its expression is elevated under ERS, CHOP induces cell apoptosis by downregulating the expression of antiapoptotic factors [30, 31]. Recent studies have suggested that ERS chaperones are in dental fluorosis and osteoblast activation in vitro [32, 33]. However, the function of ERS chaperones in vivo during osteofluorosis remains unknown.

The present study investigated the mechanism of ERS in endemic fluorosis. We used rats as an in vivo model to investigate the role of ERS chaperones in osteofluorosis and osteoblast ERS. We further investigated the relationship between excessive fluoride-induced ERS and osteoblast cell apoptosis.

## Materials and Methods

### Animals and Fluoride Exposure in Drinking Water

Four-week-old Wistar rats were provided by the Experimental Animal Center of China Medical University in Shenyang, China. The experimental protocol was in accordance with the general guidelines of the Association for Assessment and Accreditation of Laboratory Animal Care and was reviewed and approved by the Animal Care and Use Committee of Science and Technology Department of Liaoning province, China. All of the animals were housed in pairs in plastic metabolic cages within the Laboratory Animal Care. The rats were maintained on a 12:12-h light/dark cycle with an ambient temperature of 21 °C and a humidity of 40–80 %.

Forty-eight rats were randomly divided into four groups (six males and six females in each group). The control group was provided tap water that contained 0.3 mg/L fluoride. The low, middle, and high concentration groups were given sodium fluoride (NaF) water with final fluoride concentrations of 50, 100, and 150 mg/L, respectively, using methods reported previously [34–37]. A conventional rat diet containing 20 µg/g of fluoride was provided by the Experimental Animal Center of China Medical University. The animals were weighed and observed weekly for their activity, water intake, diet, and dental fluorosis. After 8 weeks of fluoride exposure, the rats were anesthetized by intraperitoneal injection of chloral hydrate [38, 39], and 5 mL of blood samples was drawn via an abdominal aorta. The blood samples were allowed to stand for 30 min, followed by centrifugation at 2000 rpm for 15 min. The serum samples were stored at –80 °C until analysis. Sections of bilateral femurs were removed and frozen at –80 °C to measure the fluoride concentration. Other sections of bilateral femurs were fixed in 4 % paraformaldehyde solution after removing soft tissues. Twenty-four hours later, 10 % EDTA solution was used for decalcification. Six weeks later, paraffin-embedded sectioning was carried out using a paraffin-sectioning machine (LKB-V, Sweden), followed by hematoxylin and eosin (H&E) staining and immunohistochemical staining.

### Fluoride Analysis

To measure the fluoride concentration in the blood, 0.2 mL of serum was mixed with 0.2 mL of total ionic strength adjustment buffer (TISAB). The mixture was transferred into a fluoride ion motor tank. The fluoride ion electrode method was used to determine the fluoride concentrations in the serum [40].

To measure the fluoride concentration in the bone, bilateral femurs were roasted in a porcelain pot at 105 °C and weighed after cooling down. Carbonation and ashing were then carried out at 560 °C for 4 h. Then, 0.1 g of ash was dissolved in 5 mL of 1 M HCl. NaOH was used to adjust the pH to 5–6, and deionized water was added to reach a total volume of 10 mL. Next, 10 mL of TISAB was added and mixed homogeneously. The same method used in the serum was used to measure the fluoride concentration in the bone [41].

### Hematoxylin and Eosin and Immunohistochemical Staining

Bone morphology was examined with H&E staining. To examine the expression of GRP78, caspase-12, XBP-1, and CHOP, sections were dewaxed and rehydrolyzed for immunohistochemistry staining using anti-GRP78/BIP, anti-caspase-12, anti-XBP1, and anti-CHOP antibodies (Abcam, Cambridge, USA; dilution ratio, 1:100). PBS instead of primary antibody was used to stain the negative control sections.

MetaMorph software (Molecular devices, USA) was used to analyze the images. Under a microscope with  $\times 400$  magnification, three fields were randomly selected on each section to measure the OD values.

#### TUNEL Assay

Sectioned bone tissue was dewaxed, rehydrolyzed, and then incubated with Proteinease K for 20 min. After being washed with PBS, the sections were incubated with 3 %  $H_2O_2$  for 30 min. TUNEL reaction mixture (Roche, USA) containing DNA terminal transferase and dNTP was added onto the sections and kept at 37 °C for 60 min. After PBS washing, a POD-labeled anti-fluorescein antibody (Roche, USA) was added onto the sections and incubated at 37 °C for 30 min. 3,3'-Diaminobenzidine (DAB) was then added to develop the signals. Hematoxylin was used for counterstaining. Reaction mixture without DNA terminal transferase was used for negative control sections. Under a microscope with  $\times 400$  magnification, three fields were randomly selected on each TUNEL staining section to calculate the percentage of positive cells (AI index).

#### Flow Cytometry

Bilateral femurs were placed in Petri dishes filled with D-Hanks solution. The periosteum and the surrounding connective tissue were removed. After being washed twice with D-Hanks solution, the bone was digested with 0.25 % trypsin at 37 °C for 15 min and then with 1 mg/mL collagenase at 37 °C for 90 min. The cells were dissociated from the bone matrix after digestion. After centrifugation of the above mixture at 1000 rpm for 5 min, the supernatant was discarded, and the cell pellet was washed with M199 media twice. The bone chips were continuously pipetted up and down several times to dissociate more osteoblasts from the loosed bone matrix. Osteoblasts were enriched and purified by the differential adhesion method [35]. Collagen I immunohistochemistry was used to identify osteoblasts. The density of purified cells was adjusted to  $1 \times 10^6$ /mL in PBS. Propidium iodide was then added to stain dead cells at 37 °C for 30 min, followed by flow cytometry analysis.  $1 \times 10^4$  cells were collected for analysis. CellQuest software (BD biosciences, San Jose, USA) was used to record the percentage of the cells in the AP region, and then, the percentage of apoptotic cells was calculated.

#### Statistical Analysis

All of the statistical analyses were performed with SPSS 13.0 software (SPSS Inc, Chicago, IL, USA). Data are expressed as mean  $\pm$  standard error of the mean and were analyzed with the two-tailed Student's *t* test. For comparison among multiple groups, one-way ANOVA was used, followed by a SNK test.  $P < 0.05$  was considered statistically significant.

## Results

### Bone Structure Was Changed After Fluoride Accumulation

To increase the concentration of fluoride in the bones and blood, drinking water containing NaF was used to feed rats. As shown in Table 1, the fluoride concentrations in both the blood and bone were increased in a dose-dependent manner.

We then examined the effect of fluoride accumulation on bone structure. Bone morphology of the femur in different groups is shown in Fig. 1. In the control group (Fig. 1a), the trabecular bone was dense and intact with uniform thickness. Osteoblast cells were arranged in a single layer on the surface of the trabecular bone. In the 50-mg/L fluoride group (Fig. 1b), the trabecular bone was denser, with increased osteoblast cells, and the trabecular mesh was smaller compared to the control group. In the 100-mg/L fluoride group (Fig. 1c), the trabecular bone was denser with increased osteoblast cells, and the trabecular mesh was smaller when compared to the 50-mg/L fluoride group. In the 150-mg/L fluoride group (Fig. 1d), the trabecular bone became disorganized. In addition, cartilage cells in the thickened layer were accumulated and disorganized. These results indicated that fluoride accumulation in the bone caused bone damage, indicating a successful skeletal fluorosis animal model.

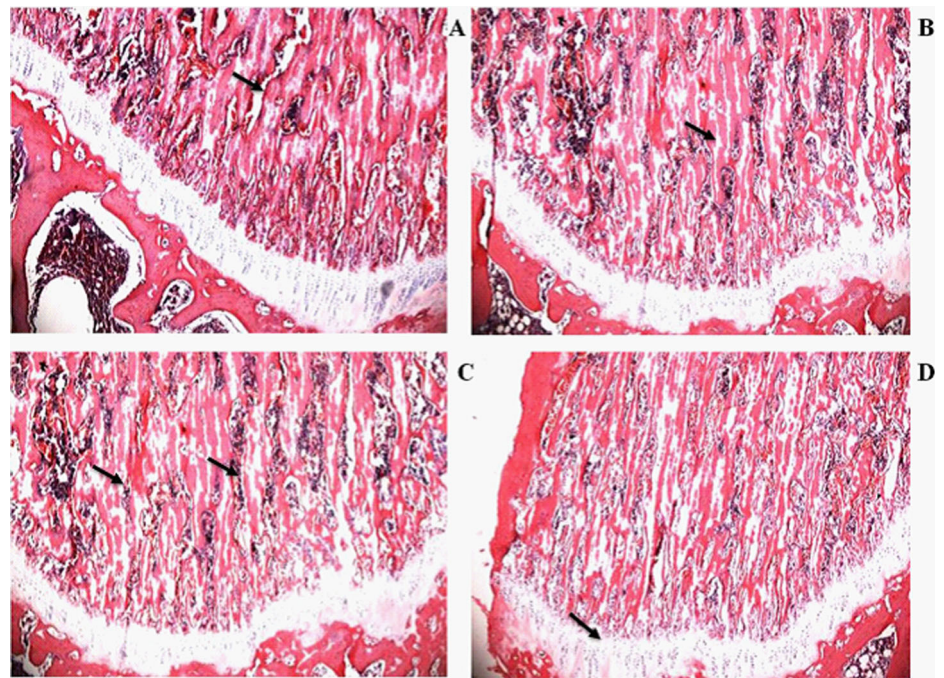
### Expression of ERS Chaperones Was Increased with the Accumulation of Fluoride in the Bones

To test whether the expression of ERS chaperones was changed in the bone fluorosis rat model, GRP78, caspase-12, XBP-1, and CHOP were detected in femur sections from different groups. In the control group, all four chaperones were expressed at a low level (Figs. 2a, 3a, 4a, 5a, and 6). In the 50-mg/L fluoride group, the expressions of all four chaperones were increased (Figs. 2b, 3b, 4b, 5b, and 6). With the increased concentration of fluoride, the expressions of the four chaperones were much higher in the 100- and 150-mg/L fluoride groups than those of the other groups (Figs. 2c, d,

**Table 1** Blood and bone fluoride concentrations in rats following exposure to different concentrations of fluoride ( $\bar{x} \pm s$ ,  $n=12$ )

Group	Blood fluoride $\mu\text{g/mL}$	Bone fluoride $\mu\text{g/mg}$
Control	0.130 $\pm$ 0.043	463.097 $\pm$ 71.647
50 mg/L	0.175 $\pm$ 0.025	893.628 $\pm$ 67.748
100 mg/L	0.230 $\pm$ 0.036	1001.111 $\pm$ 34.121
150 mg/L	0.313 $\pm$ 0.042	1248.152 $\pm$ 77.131
<i>F</i>	11.234	217.337
<i>P</i>	<0.05	<0.05

**Fig. 1** Bone structures in rats following fluoride accumulation (H&E staining). **a** The control group. *Arrowhead* indicates the uniform thickness of trabecular bones. **b** The 50-mg/L fluoride sodium group. *Arrowhead* indicates increased and dense arranged trabecular bone. **c** The 100-mg/L fluoride sodium group. *Arrowhead* indicates increased osteoblasts on the surface of trabecular bone. **d** The 150-mg/L fluoride sodium group. *Arrowhead* indicates accumulated and disorganized cartilage cells. Magnification  $\times 200$



3c, d, 4c, d, 5c, d, and 6;  $P < 0.05$ ). These results indicated that accumulation of fluoride in osteoblasts could induce the expression of ERS chaperones in vivo.

#### Cell Apoptosis Was Induced After Accumulation of Fluoride in the Bone

As shown in Table 2, the mean percentage of apoptotic osteoblast cells in the high fluoride group was much

higher than that in the middle and low fluoride exposure groups ( $P < 0.05$ ). TUNEL assay showed that rats in the high fluoride group had more apoptotic osteoblasts than those in the middle and low fluoride groups. FACSscan analysis showed that the percentage of apoptotic osteoblasts was higher in the high fluoride group than that in the middle and low fluoride groups. These results suggested that an accumulation of fluoride in bone caused osteoblast apoptosis.

**Fig. 2** Expression of GRP78 in rat osteoblasts following exposure to various concentrations of fluoride. **a** The control group. *Arrow* indicates the low expression of GRP78 in osteoblasts. **b** The 50-mg/L fluoride group. *Arrowhead* indicates the increased expression of GRP78 in osteoblasts. **c** The 100-mg/L fluoride group. *Arrowhead* indicates the stronger signal of GRP78 in osteoblasts. **d** The 150-mg/L fluoride group. *Arrowhead* indicates the stronger signal of GRP78 in osteoblasts. Magnification  $\times 400$

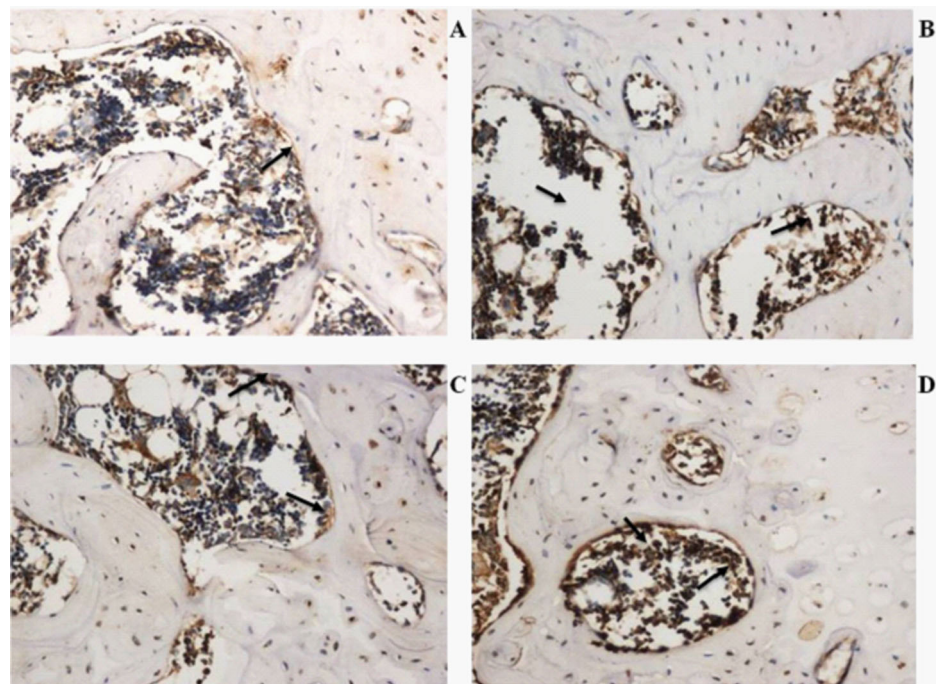
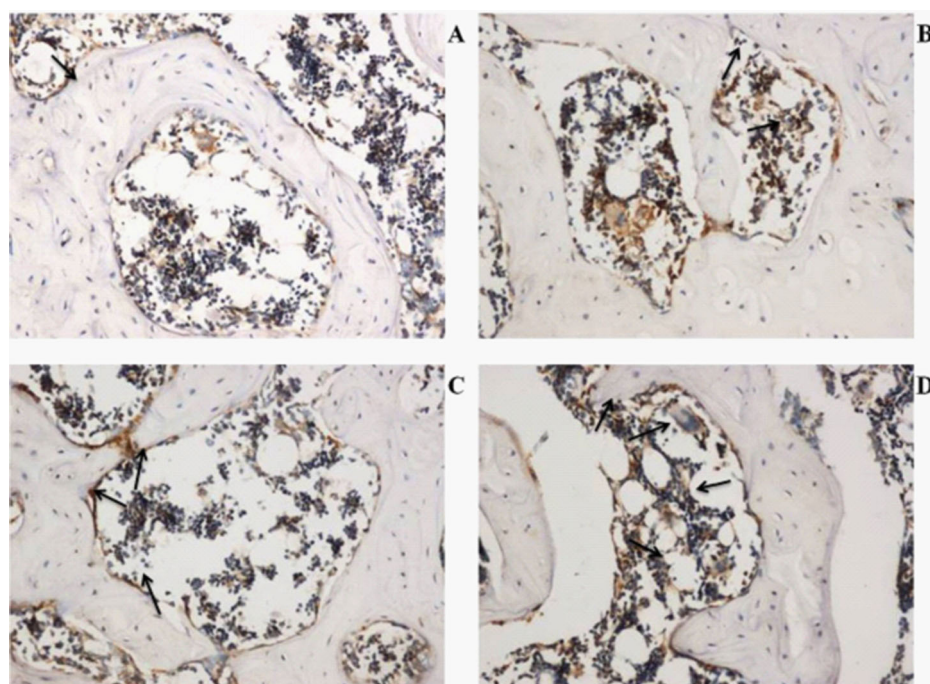


**Fig. 3** Expression of caspase-12 in rat osteoblasts following exposure to various concentrations of fluoride. **a** The control group. *Arrow* indicates the low expression of caspase-12 in osteoblasts. **b** The 50-mg/L fluoride group. *Arrowhead* indicates the increased expression of caspase-12 in osteoblasts. **c** The 100-mg/L fluoride group. *Arrowhead* indicates the stronger signal of caspase-12 in osteoblasts. **d** The 150-mg/L fluoride group. *Arrowhead* indicates the stronger signal of caspase-12 in osteoblasts. Magnification  $\times 400$



## Discussion

The present study showed that ERS could be induced *in vivo* by fluoride overload in the bone. Our results also suggested that the accumulation of fluoride in the bone induced osteoblast apoptosis.

ERS has been extensively studied in pancreatic, cardiac, and neural diseases [17, 25, 27, 29], but not in endemic fluorosis. Studies on endemic fluorosis have mainly focused

on *in vitro* cultured cells. Wei et al. [32] found that excessive fluoride induced ERS in ameloblasts and affected the secretion of enamel matrix, suggesting a role of ERS in the formation of dental fluorosis. Zhou et al. [33] found that BIP and CHOP expressions were significantly increased due to excessive fluoride in the culture media of osteoblasts, suggesting that fluoride could induce ERS in osteoblasts and activate UPR. Our current study showed for the first time that fluoride could induce ERS and cause osteoblast apoptosis *in vivo*.

**Fig. 4** Expression of XBP-1 in rat osteoblasts following exposure to various concentrations of fluoride. **a** The control group. *Arrow* indicates the low expression of XBP-1 in osteoblasts. **b** The 50-mg/L fluoride group. *Arrowhead* indicates the increased expression of XBP-1 in osteoblasts. **c** The 100-mg/L fluoride group. *Arrowhead* indicates the stronger signal of XBP-1 in osteoblasts. **d** The 150-mg/L fluoride group. *Arrowhead* indicates the stronger signal of XBP-1 in osteoblasts. Magnification  $\times 400$

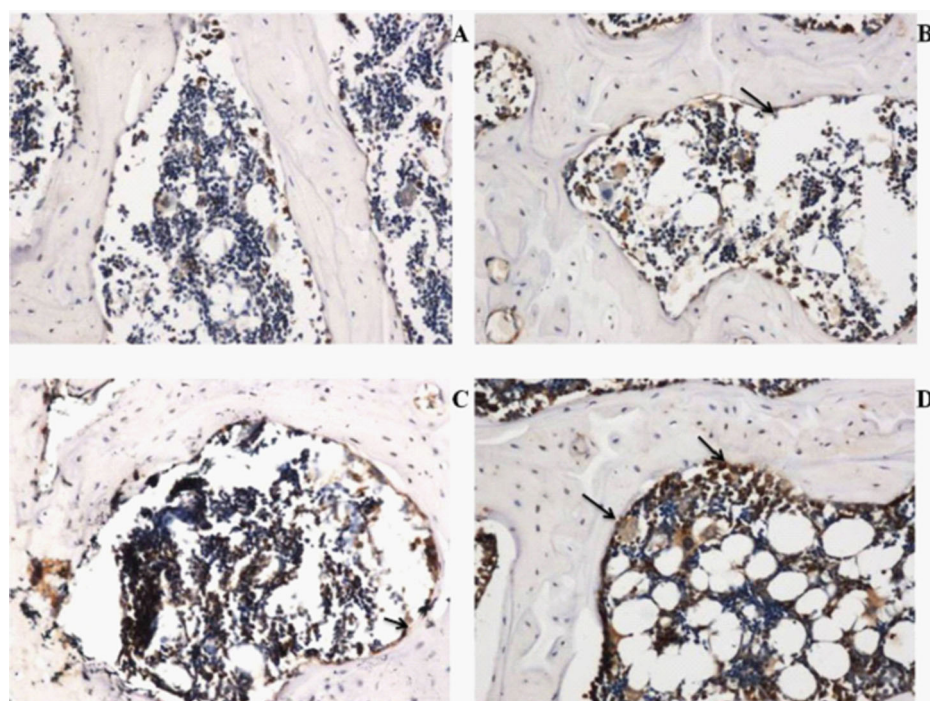
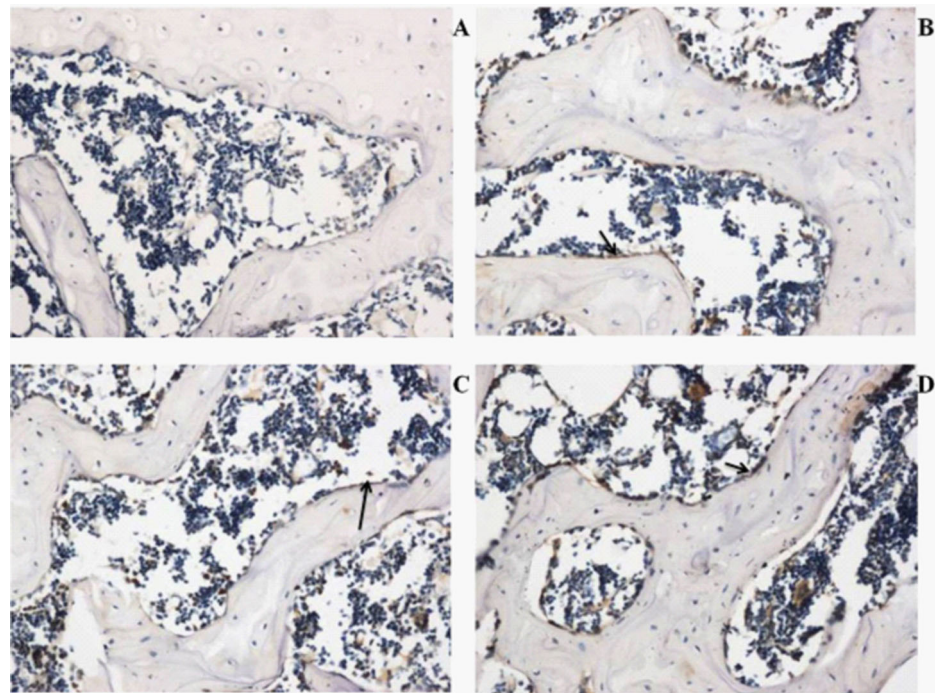


**Fig. 5** Expression of XBP-1 in rat osteoblasts following exposure to various concentrations of fluoride. **a** The control group. *Arrow* indicates the low expression of CHOP in osteoblasts. **b** The 50-mg/L fluoride group. *Arrowhead* indicates the increased expression of CHOP in osteoblasts. **c** The 100-mg/L fluoride group. *Arrowhead* indicates the stronger signal of CHOP in osteoblasts. **d** The 150-mg/L fluoride group. *Arrowhead* indicates the stronger signal of CHOP in osteoblasts. Magnification  $\times 400$



In the present study, the rats were exposed to different concentrations of NaF in drinking water. We found that the rat blood and bone fluoride concentrations were significantly increased in a dose-dependent manner, suggesting a successful rat fluoride poisoning model. We used this model to determine the role of ERS chaperones in fluoride toxicity. Our results showed that the expression of ERS chaperones in the fluoride groups was significantly higher than that in the control group, indicating a role of ERS in the formation of osteofluorosis. GRP78 is very sensitive to minor changes of the ER. Our immunohistochemical results showed that the expression of GRP78 was significantly higher in the high fluoride group than that in the middle and low fluoride groups, indicating that ERS played a role in the pathogenesis of osteofluorosis. High fluoride can activate the ER membrane

receptor and promote its dissociation with GRP78. This process may be the initiation of ERS. Dhahbi et al. [24] found that the expression of GRP78 in cultured rat hepatocytes was increased when the concentration of glucose was  $<1.0$  mmol/L but decreased when the concentration was in the range of 1.0~4.5 mmol/L. Since the fluoride concentrations tested in our current study were relatively limited, we cannot rule out the possibility of an inhibitory effect on the GRP78 expression with higher concentrations of fluoride.

ERS activation induces downstream molecules. XBP1 plays an important role in restoring ER homeostasis and preventing cell apoptosis [13]. Our immunohistochemical results showed that the expression of XBP1 was increased with increasing concentrations of fluoride. These findings are consistent with the report by Zhou et al. [33], suggesting that

**Fig. 6** Expression levels of ERS chaperones in the bone. Expressions of all four chaperones were increased with increasing concentrations of fluoride ( $P < 0.05$ )

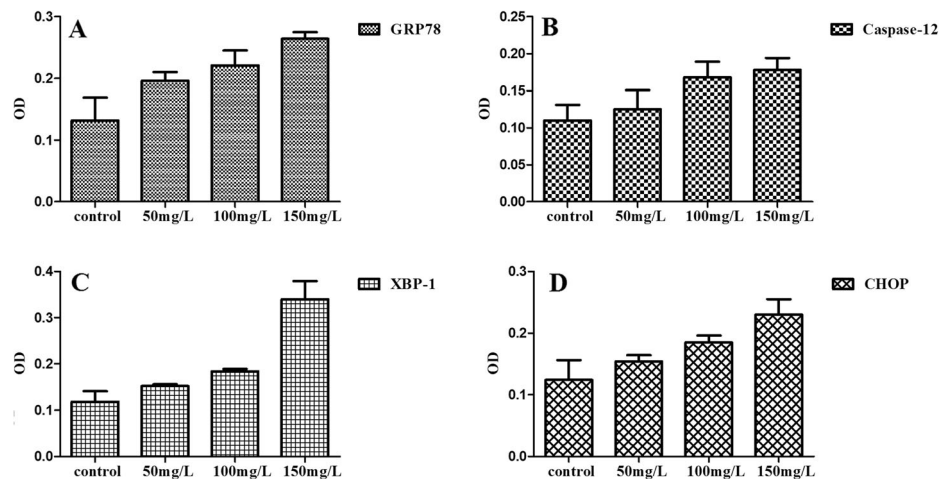


**Table 2** Osteoblast apoptosis in rats following exposure to different concentrations of fluoride ( $\bar{x} \pm s$ ,  $n=12$ )

Groups	TUNEL (AI value)	% apoptosis
Control	9.33±1.53	6.68±0.90
50 mg/L	21.13±6.34*	8.08±1.24
100 mg/L	68.38±7.37*	12.42±1.76
150 mg/L	92.10±7.00*	25.34±0.69*

\*  $P < 0.05$ , compared with the control group

high expression of XBP1 may prevent osteoblast apoptosis and help restore the osteoblast homeostasis following treatment with a high concentration of fluoride.

Nakagawa et al. [42] found that ERS-induced apoptosis was decreased in caspase-12 knockout mice. In this study, the expression of caspase-12 was increased with increasing concentrations of fluoride. In addition, TUNEL assay indicated increased apoptosis in the high fluoride group compared to the other groups. Taken together, these results suggested that the expression of caspase-12 was associated with osteoblast apoptosis and that inhibition of caspase-12 might block fluoride-induced apoptosis in osteoblasts.

Our current study also found that the expression of CHOP was increased with increasing concentrations of fluoride in the drinking water. This finding further suggested that fluoride could induce ERS in osteoblasts and that increased ERS might cause osteoblast apoptosis. Together with the results of caspase-12, our results indicated that osteoblast apoptosis was induced by multiple signaling pathways.

Osteoblasts are highly sensitive target cells for fluoride poisoning. Our previous studies found that 2 mmol/L of fluoride induced apoptosis in rat osteoblasts in vitro [36]. Ren et al. [43] found that 0.5 mg/L of fluoride caused osteoblast apoptosis. In our current study, apoptosis was observed in a fluorosis rat model. TUNEL assay results showed that osteoblast apoptosis was closely related with the fluoride concentration. These findings are consistent with the report of Yan et al. [28]. Osteoblast morphology can change in the early stages of apoptosis. At the late stage of apoptosis, the arrangement of osteoblasts can become loose due to cell death. This may explain the abnormal structures we observed in this study following H&E staining of the bones of rats with osteofluorosis. In this study, FACScan analysis showed that the percentage of apoptotic osteoblasts was higher in the high fluoride group than that in the middle and low fluoride groups. These results indicated that high fluoride levels in rat bone could induce ERS and osteoblast apoptosis. Additionally, the osteofluorosis model described in this study might provide a basis for further study on the mechanism of fluoride-induced bone damage.

In summary, our results suggested that excessive fluoride caused ERS in osteoblasts and induced apoptosis. Caspase-12

and CHOP were activated in the process of UPR and played critical roles in ERS-induced osteoblast apoptosis. Our results may provide new strategies for the prevention and treatment of endemic fluorosis in the future.

**Acknowledgments** This study was supported by a grant from the National Natural Science Foundation of China (No. 81072245) and the Natural Science Foundation of Liaoning Province (No. 20102278).

**Conflicts of Interest** The authors declare that there are no conflicts of interest.

## References

1. Aliasgharpour M, Rahnamaye FM (2013) Trace elements in human nutrition: a review. *Int J Med Invest* 2(3):115–128
2. Buchancová J, Poláček H, Hudečková H, Murajda L, Osina O, Valachová J (2008) Skeletal fluorosis from the point of view of an occupational exposure to fluorides in former Czechoslovakia. *Interdiscip Toxicol* 1(2):193–197
3. Jha SK, Mishra VK, Sharma DK, Damodaran T (2011) Fluoride in the environment and its metabolism in humans. *Rev Environ Contam Toxicol* 211:121–142
4. Harding MA, O'Mullane DM (2013) Water fluoridation and oral health. *Acta Med Acad* 42:131–139
5. Dhar V, Bhatnagar M (2009) Physiology and toxicity of fluoride. *Indian J Dent Res* 20:350–355
6. Everett ET (2011) Fluoride's effects on the formation of teeth and bones, and the influence of genetics. *J Dent Res* 90:552–560
7. Debinski A, Nowicka G (2004) Effect of sodium fluoride on ectopic induction of bone tissue. *Ann Acad Med Stetin* 50:23–27
8. Nair M, Belak ZR, Ovsenek N (2011) Effects of fluoride on expression of bone-specific genes in developing *Xenopus laevis* larvae. *Biochem Cell Biol* 89:377–386
9. Krishnamachari KA (1986) Skeletal fluorosis in humans: a review of recent progress in the understanding of the disease. *Prog Food Nutr Sci* 10:279–314
10. Fujita T, Palmieri GMA (2000) Calcium paradox disease: calcium deficiency prompting secondary hyperparathyroidism and cellular calcium overload. *Bone Miner Metab* 18(3):109–125
11. Hua K, Zhao H, Huang M, Li GS (2003) Effects of fluoride on ionized calcium and calcium channel in osteoblast-like cell in vitro. *Zhongguo Ying Yong Sheng Li Xue Za Zhi* 19:179–181
12. Bary EL (2000) Expression of mRNA for the alpha 1 subunit of voltage-gated calcium channels in human osteoblast like cell line and normal human osteoblasts. *Calcif Tissue Int* 66(2):145–150
13. Wang X, Eno CO, Altman BJ, Zhu Y, Zhao G, Olberding KE, Rathmell JC, Li C (2011) ER stress modulates cellular metabolism. *Biochem J* 435(1):285–296
14. Verkhatsky A, Toescu EC (2003) Endoplasmic reticulum Ca<sup>2+</sup> homeostasis and neuronal death. *J Cell Mol Med* 7(4):351–361
15. Smaili SS, Pereira GJ, Costa MM, Rocha KK, Rodrigues L, do Carmo LG, Hirata H, Hsu YT (2013) The role of calcium stores in apoptosis and autophagy. *Curr Mol Med* 13:252–265
16. Mahoney E, Byrd JC, Johnson AJ (2013) Autophagy and ER stress play an essential role in the mechanism of action and drug resistance of the cyclin-dependent kinase inhibitor flavopiridol. *Autophagy* 9(3):434–435
17. Hetz C, Chevet E, Harding HP (2013) Targeting the unfolded protein response in disease. *Nat Rev Drug Discov* 12:703–719

18. Kaneko M (2012) Molecular pharmacological studies on the protection mechanism against endoplasmic reticulum stress-induced neurodegenerative disease. *Yakugaku Zasshi* 132(12):1437–1442
19. Hamamura K, Yokota H (2007) Stress to endoplasmic reticulum of mouse osteoblasts induces apoptosis and transcriptional activation for bone remodeling. *FEBS Lett* 581(9):1769–1774
20. Higa A, Chevet E (2012) Redox signaling loops in the unfolded protein response. *Cell Signal* 24:1548–1555
21. Hammadi M, Oulidi A, Gackière F, Katsogiannou M, Slomianny C, Roudbaraki M, Dewailly E, Delcourt P, Lepage G, Lotteau S, Ducreux S, Prevarskaya N, Van Coppenolle F (2013) Modulation of ER stress and apoptosis by endoplasmic reticulum calcium leak via translocon during unfolded protein response: involvement of GRP78. *FASEB J* 27:1600–1609
22. Jwa M, Chang P (2012) PARP16 is a tail-anchored endoplasmic reticulum protein required for the PERK- and IRE1 $\alpha$ -mediated unfolded protein response. *Nat Cell Biol* 14(11):1223–1230
23. Pfaffenbach KT, Amy S (2011) The critical role of GRP78 in physiologic and pathologic stress. *Curr Opin Cell Biol* 23(2):150–156
24. Dhahbi JM, Mote PL, Tillman JB, Walford RL, Spindler SR (1997) Dietary energy tissue-specifically regulates endoplasmic reticulum chaperone gene expression in the liver of mice. *J Nutr* 127(9):1758–1764
25. Malhi H, Kaufman RJ (2011) Endoplasmic reticulum stress in liver disease. *J Hepatol* 54:795–809
26. Jurczak MJ, Lee AH, Jornayvaz FR, Lee HY, Birkenfeld AL, Guigni BA, Kahn M, Samuel VT, Glimcher LH, Shulman GI (2012) Dissociation of inositol-requiring enzyme (IRE1 $\alpha$ )-mediated c-Jun N-terminal kinase activation from hepatic insulin resistance in conditional X-box-binding protein-1 (XBP1) knock-out mice. *J Biol Chem* 287(4):2558–2567
27. Liu D, Zhang M, Yin H (2013) Signaling pathways involved in endoplasmic reticulum stress-induced neuronal apoptosis. *Int J Neurosci* 123(3):155–162
28. Yan X, Feng C, Chen Q, Li W, Wang H, Lv L, Smith GW, Wang J (2009) Effects of sodium fluoride treatment in vitro on cell proliferation, apoptosis and caspase-3 and caspase-9 mRNA expression by neonatal rat osteoblasts. *Arch Toxicol* 83:451–458
29. Moriya S, Miyazawa K, Kawaguchi T, Che XF, Tomoda A (2011) Involvement of endoplasmic reticulum stress-mediated CHOP (GADD153) induction in the cytotoxicity of 2-aminophenoxazine-3-one in cancer cells. *Int J Oncol* 39(4):981–988
30. Komatsu S, Miyazawa K, Moriya S, Takase A, Naito M, Inazu M, Kohno N, Itoh M, Tomoda A (2012) Clarithromycin enhances bortezomib-induced cytotoxicity via endoplasmic reticulum stress-mediated CHOP (GADD153) induction and autophagy in breast cancer cells. *Int J Oncol* 40(4):1029–1039
31. Bromati CR, Lellis-Santos C, Yamanaka TS, Nogueira TC, Leonelli M, Caperuto LC, Gorjão R, Leite AR, Anhô GF, Bordin S (2011) UPR induces transient burst of apoptosis in islets of early lactating rats through reduced AKT phosphorylation via ATF4/CHOP stimulation of TRB3 expression. *Am J Physiol Regul Integr Comp Physiol* 300(1):92–100
32. Wei W, Gao Y, Wang C, Zhao L, Sun D (2013) Excessive fluoride induces endoplasmic reticulum stress and interferes enamel proteinases secretion. *Environ Toxicol* 28(6):332–341
33. Zhou YL, Shi HY, Li XN, Lv P, Li GS, Liu QY, Xu H (2013) Role of endoplasmic reticulum stress in aberrant activation of fluoride-treated osteoblasts. *Biol Trace Elem Res* 154(3):448–456
34. Zhang Y, Liang YJ, Guo XY, Li X (2005) The effect of high dose fluoride on the rat offspring osteoblasts which ingested by female rats. *Wei Sheng Yan Jiu* 34(1):29–32
35. Zhang Y, Sun X, Sun GF, Liu S, Wang L (2006) DNA damage induced by fluoride in rat osteoblasts. *Fluoride* 39(3):191–194
36. Zhang Y, Sun G, Jin Y, Wang Y (2003) Effects of fluoride on cell cycle and apoptosis in cultured osteoblasts of rats. *Wei Sheng Yan Jiu* 32(5):432–433
37. Zhang Y, Sun GF, Jin YP, Wang Y (2003) Effects of fluoride on proliferation and differentiation of osteoblast. *Chin J Public Health* 19(4):411–413
38. Zhou R, Zaki AE, Eisenmann DR (1996) Morphometry and autoradiography of altered rat enamel rat enamel protein processing due to chronic exposure to fluoride. *Arch Oral Biol* 41(8–9):739–747
39. Shore RC, Robinson C, Kirkham J, Herold RC (1993) An immunohistochemical study of the effects of fluoride on enamel development in the rat incisor. *Arch Oral Biol* 38(7):607–610
40. Lubkowska A, Chlubek D, Machoy-Mokrzyniska A (2006) The effect of alternating administration of aluminum chloride and sodium fluoride in drinking water on the concentration of fluoride in serum and its content in bones of rats. *Ann Acad Med Stetin* 52(Suppl 1):67–71
41. Tu J, Liu K, Song Y, Zhang Y, Cui C, Lu C (2011) Interactive effect of fluoride burden with calcitonin receptor gene polymorphisms on the risk of F bone injury. *Int Arch Occup Environ Health* 84(5):533–538
42. Nakagawa T, Zhu H, Morishima N, Li E, Xu J, Yankner BA, Yuan J (2000) Caspase-12 mediates endoplasmic-reticulum-specific apoptosis and cytotoxicity by amyloid $\beta$ . *Nature* 403(6765):98–103
43. Ren G, Ferreri M, Wang Z, Su Y, Han B, Su J (2011) Sodium fluoride affects proliferation and apoptosis through insulin-like growth factor I receptor in primary cultured mouse osteoblasts. *Biol Trace Elem Res* 144:914–923